ResearchGate

See discussions, stats, and author profiles for this publication at: https://www.researchgate.net/publication/223637457

NDWI?A Normalized Difference Water Index for Remote Sensing of Vegetation Liquid Water from Space

Article *in* Proceedings of SPIE - The International Society for Optical Engineering · December 1996

DOI: 10.1016/S0034-4257(96)00067-3

CITATIONS
6,314

READS
9,760

1 author:

Bo-Cai Gao
United States Naval Research Laboratory
193 PUBLICATIONS **16,958** CITATIONS

SEE PROFILE

All content following this page was uploaded by Bo-Cai Gao on 10 January 2022.

The user has requested enhancement of the downloaded file.

ELSEVIER

NDWI—A Normalized Difference Water Index for Remote Sensing of Vegetation Liquid Water From Space

*Bo-Cai Gao**

The normalized difference vegetation index (NDVI) has been widely used for remote sensing of vegetation for many years. This index uses radiances or reflectances from a red channel around 0.66 μm and a near-IR channel around 0.86 μm. The red channel is located in the strong chlorophyll absorption region, while the near-IR channel is located in the high reflectance plateau of vegetation canopies. The two channels sense very different depths through vegetation canopies. In this article, another index, namely, the normalized difference water index (NDWI), is proposed for remote sensing of vegetation liquid water from space. NDWI is defined as (ρ(0.86 μm) − ρ(1.24 μm)) / (ρ(0.86 μm) + ρ(1.24 μm)), where ρ represents the radiance in reflectance units. Both the 0.86-μm and the 1.24-μm channels are located in the high reflectance plateau of vegetation canopies. They sense similar depths through vegetation canopies. Absorption by vegetation liquid water near 0.86 μm is negligible. Weak liquid absorption at 1.24 μm is present. Canopy scattering enhances the water absorption. As a result, NDWI is sensitive to changes in liquid water content of vegetation canopies. Atmospheric aerosol scattering effects in the 0.86–1.24 μm region are weak. NDWI is less sensitive to atmospheric effects than NDVI. NDWI does not remove completely the background soil reflectance effects, similar to NDVI. Because the information about vegetation canopies contained in the 1.24-μm channel is very different from that contained in the red channel near 0.66 μm, NDWI should be considered as an independent vegetation index. It is complementary to, not a substitute for NDVI. Laboratory-measured reflectance spectra of stacked green leaves, and spectral imaging data acquired with Airborne Visible Infrared Imaging Spectrometer (AVIRIS) over Jasper Ridge in California and the High Plains in northern Colorado, are used to demonstrate the usefulness of NDWI. Comparisons between NDWI and NDVI images are also given. © Elsevier Science Inc., 1996

INTRODUCTION

The normalized difference vegetation index (NDVI) is the most widely used index for remote sensing of vegetation in the past two decades. It is equal to $(\rho_{NIR} - \rho_{RED}) / (\rho_{NIR} + \rho_{RED})$, where ρ_{RED} is the radiance (in reflectance units) of a red channel near 0.66 μm, and ρ_{NIR} the radiance (in reflectance units) of a near-IR channel around 0.86 μm. This index has been used in many applications, including estimation of crop yields and end-of-season above-ground dry biomass (Tucker et al., 1986). The two channels used in NDVI sense through different depths of vegetation canopies. The near-IR channel can see roughly eight leaf layers, while the red channel sees only one leaf layer or less (Lillesaeter, 1982) because of the strong chlorophyll absorption near 0.67 μm. In spite of its usefulness, NDVI is known to be saturated when applied to images over areas having leaf area index of 3 or greater. Numerous other vegetation indices with varying complexity have been developed using the same set of near-IR and red channels during the past decade. These indices do not have nearly the same popularity as that of NDVI. The recently developed Atmospherically Resistant Vegetation Index (ARVI) (Kaufman and Tanré, 1992) used not only the near-IR and red channels, but also a blue channel near 0.47 μm. This index has self-correction properties for the atmospheric effect.

* Joint Center for Earth Systems Sciences, NASA Goddard Space Flight Center, Greenbelt, Maryland

Address correspondence to B.-C. Gao, Remote Sensing Division, Code 7212, Naval Research Laboratory, 4555 Overlook Ave., SW, Washington, DC 20375.

Received 30 April 1995; revised 6 April 1996.

REMOTE SENS. ENVIRON. 58:257–266 (1996)
©Elsevier Science Inc., 1996
655 Avenue of the Americas, New York, NY 10010

0034-4257/96/$15.00
PII S0034-4257(96)00067-3

Remote sensing of vegetation liquid water has important applications in agriculture and forestry. In this article, a normalized difference water index (NDWI) that uses two near-IR channels centered approximately at 0.86 μm and 1.24 μm for remote sensing of vegetation liquid water from space is proposed. The 1.24-μm channel has not been used previously in the formation of vegetation indices. Preliminary research on this index was reported in a scientific conference (Gao, 1995).

BACKGROUND

The spectral features in reflectance spectra of green vegetation in the 0.9–2.5 μm region are dominated by liquid water absorption, and also weakly affected by absorption due to other biochemical components (Gao and Goetz, 1994). Tucker (1980) first suggested that the 1.55–1.75 μm spectral interval (the bandpass of Landsat TM Channel 5) was the best-suited band in the 0.7–2.5 μm region for monitoring plant canopy water status from space. Some experimental studies showed that the reflectances for certain types of vegetation over the bandpass of TM Channel 5 increased as leaf water content decreased (e.g., Cibula et al., 1992). A number of broad-channel ratio and combination techniques (Jackson et al., 1983; Hunt et al., 1987) using TM Channel 4 (0.76–0.90 μm) and TM Channel 5 were proposed for remote sensing of plant water status. Several studies using broad-channel ratio techniques failed to detect plant water status change within a biologically meaningful range (Hunt and Rock, 1989; Pierce et al., 1990; Bowman, 1990).

Imaging spectrometers acquire images in many contiguous channels such that, for each picture element (pixel), a reflectance or emittance spectrum without gaps is measured for the wavelength region covered (Goetz et al., 1985). Using spectrum-matching technique, both the equivalent water thickness (EWT) and information related to biochemical components of vegetation canopies have been derived from airborne imaging spectrometer data (Gao and Goetz, 1995).

Some of the future satellite instruments, such as the Moderate Resolution Imaging Spectrometer (MODIS) (Salomonson et al., 1989) and Landsat TM8, will have many narrow, discrete channels in the 0.4–2.5 μm solar spectral region with signal to noise ratios greater than 100. Because these instruments do not have contiguous spectral coverages, spectrum-matching techniques are obviously not suitable for the derivation of liquid water content of vegetation from data acquired with these instruments. However, it is still possible to get some information about vegetation liquid water from these data using, for example, the normalized difference water index (NDWI) described below.

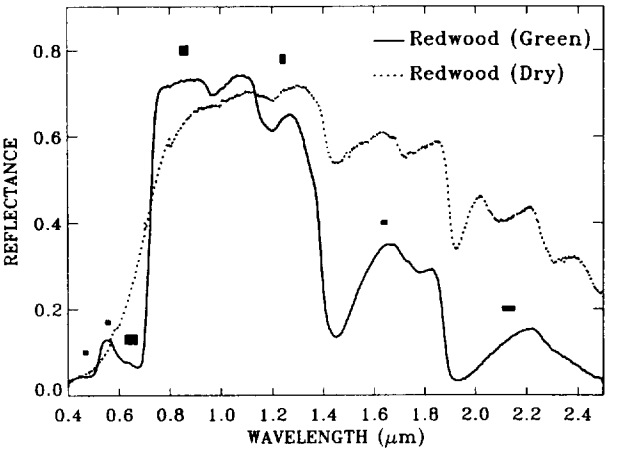

Figure 1. Examples of laboratory-measured green and dry vegetation reflectance spectra (Elvidge, 1990). The positions and widths of seven MODIS channels are marked with thick horizontal bars in this figure.

THE FORMATION OF NDWI

The normalized difference water index (NDWI) proposed here uses two near-IR channels; one centered approximately at 0.86 μm, and the other at 1.24 μm. Following the simplicity of NDVI, NDWI is defined as

$$\mathrm{NDWI} = \{\rho(0.86\,\mu\mathrm{m}) - \rho(1.24\,\mu\mathrm{m})\} / \{\rho(0.86\,\mu\mathrm{m}) + \rho(1.24\,\mu\mathrm{m})\}, \quad (1)$$

where $\rho(\lambda)$ is apparent reflectance, and λ is wavelength. $\rho(\lambda)$ is equal to $\pi\, L(\lambda) / [\cos(\theta_0)\, E_0(\lambda)]$ with $L(\lambda)$, θ_0, and $E_0(\lambda)$ being the measured radiance, the solar zenith angle, and the solar irradiance above the earth atmosphere, respectively. In order to show that NDWI can be useful for remote sensing vegetation liquid water status from space, the reflectance properties of green vegetation, dry vegetation and soils, and the absorption and scattering properties of atmospheric gases and aerosols are described below.

Green and Dry Vegetation

Sample laboratory measurements of green and dry vegetation reflectance spectra are shown in Figure 1. The positions and widths of seven MODIS channels are also illustrated in this figure. Because both the 0.86-μm and 1.24-μm channels are located in the high reflectance plateau, the vegetation scattering properties for the two channels are expected to be about the same. Two liquid water absorption features centered, respectively, at 0.98 μm and 1.20 μm in the green vegetation spectrum are small. Although the 1.24-μm channel is off the center of the 1.20-μm liquid water feature, liquid water absorptions at both wavelengths are comparable. The NDWI value for this green vegetation spectrum is 0.064 (positive). The reflectances of the dry vegetation in the

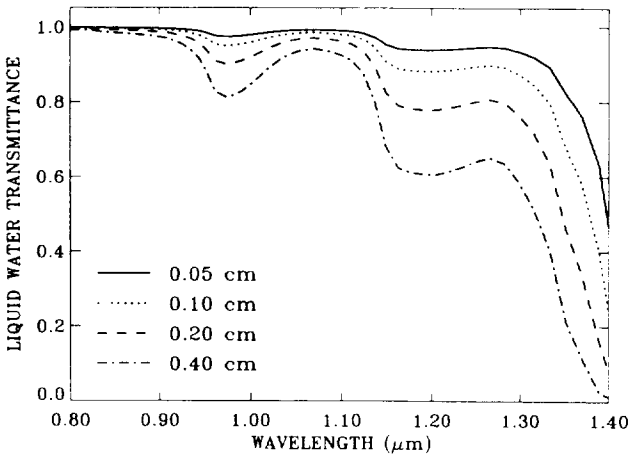

Figure 2. Liquid water transmittances for water thicknesses of 0.05 cm, 0.1 cm, 0.2 cm, and 0.5 cm (from top to bottom).

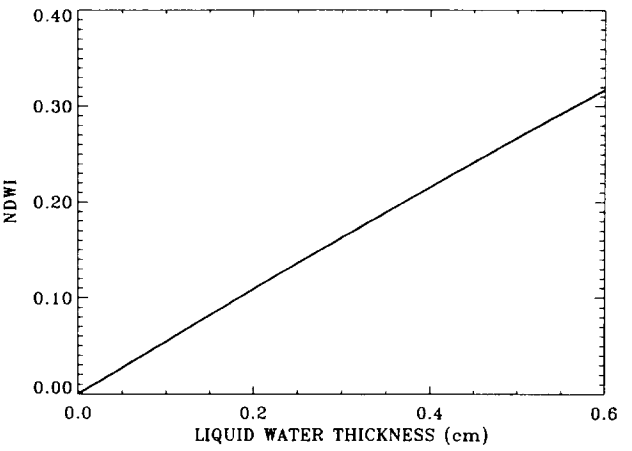

Figure 3. Sensitivity of NDWI to liquid water thickness.

0.8–1.3 μm region generally increase with wavelength, except near 1.20 μm, where a weak cellulose absorption band is present. The cellulose absorption effect at 1.24 μm is much smaller than that at 1.20 μm. Therefore, the use of a narrow channel at 1.24 μm in the formation of NDWI largely avoids the cellulose absorption effects on NDWI. The value of NDWI for the dry vegetation spectrum is −0.056 (negative). In general, NDWI value for green vegetation is positive due to the weak liquid water absorption near 1.24 μm.

Liquid water absorption in the 1.5–2.5 μm region for a green vegetation spectrum is significantly stronger than that in the 0.9–1.3 μm region, as seen from Figure 1. The reflectance spectra in the 1.5–2.5 μm region saturate when leaf area index reaches 4 or greater (Lillesaeter, 1982). On the other hand, because liquid water absorption in the 0.9–1.3 μm is weak, the vegetation spectrum in this region is sensitive to changes in leaf water content until leaf area index reaches 8 (Lillesaeter, 1982). This sensitivity to liquid water changes is illustrated in Figure 2, in which the liquid water transmittances for water thicknesses of 0.05 cm, 0.1 cm, 0.2 cm, and 0.4 cm are shown. These transmittance spectra were calculated using water refractive indices compiled by Palmer and Williams (1974). Figure 3 shows NDWI as a function of liquid water thickness. NDWI varies almost linearly with liquid water thickness. Because the 1.24-μm channel has similar vegetation scattering properties as the 0.86-μm channel, and because the 1.24-μm channel is sensitive to liquid water changes (see Fig. 2), NDWI is expected to be sensitive to vegetation liquid water changes.

Soils

Some land surface areas are covered partially by vegetation. The influence of soil background on NDWI must be studied. Reflectance spectra for a variety of natural surfaces have been compiled by Bowker et al. (1985). Typical soil reflectances increase with wavelength in the 0.8–1.3 μm region. The reflectances of these soils, including very wet soils, do not show liquid water absorption bands centered near 0.98 μm and 1.20 μm. Figure 4a shows a scatter diagram between reflectance at 1.24 μm and that at 0.86 μm for over 500 wet soils (Stoner and Baumgardner, 1980), A straight 1:1 line is also shown in this figure. Figure 4b is similar to Figure 4a, except for approximately 130 drier soils. Because reflectances at 1.24 μm for most wet and dry soils are greater than those at 0.86 μm, NDWI values are expected to be negative for most bare soils.

Figures 5a and 5b show more explicitly the soil effects on NDWIs. In Figure 5a, a scatter diagram between NDWI and 0.86-μm reflectance for the wet soils is shown. Figure 5b is similar to Figure 5a, except for the drier soils. More than 98% of soils have negative NDWIs. Only a few soils have positive NDWIs. Both scatter diagrams show a tendency that, as the 0.86-μm reflectance increases, NDWI increases and the absolute value of NDWI decreases. The scatter diagrams demonstrate that NDWI does not remove completely the background soil effects.

In order to examine the soil effects on NDWI under the condition of partial vegetation coverage, NDWIs for areas with mixtures of soils and vegetation are studied. The vegetation considered here is one kind of conifer forest. The 0.86-μm reflectance for the vegetation is 0.294, and the 1.24-μm reflectance, 0.261. The reflectances are derived from remote sensing data acquired over the forest with atmospheric effects being removed. The NDWI for this vegetation with 100% vegetation cover is approximately 0.06. NDWIs for all the wet and dry soils mixed with this vegetation having different area fractions are calculated. Figure 6 shows the mean

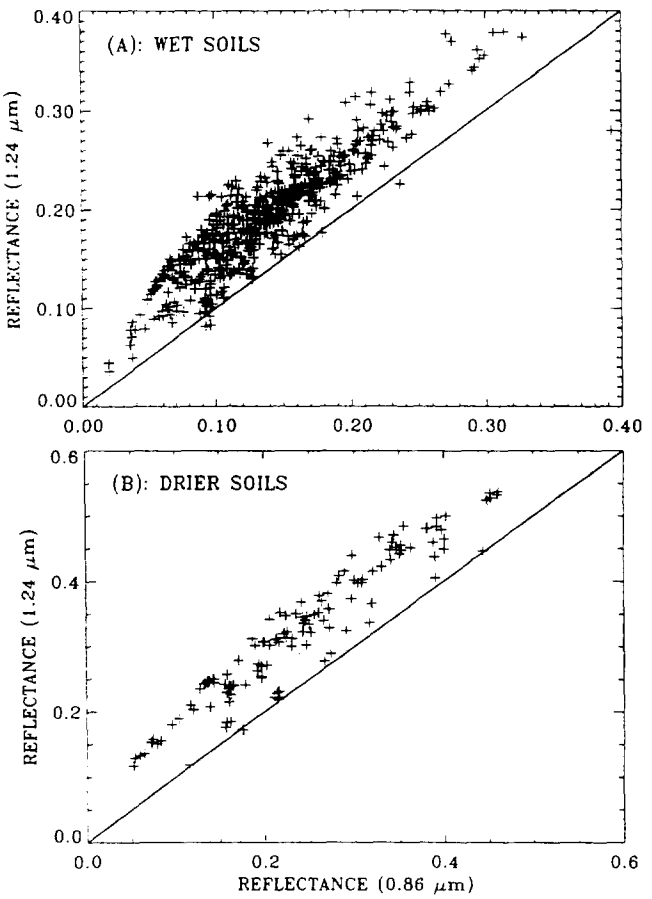

Figure 4. a) A scatter diagram between reflectance at 1.24 μm and that at 0.86 μm for over 500 wet soils (Stoner and Baumgardner, 1980), and b) similar to a), but for approximately 130 drier soils.

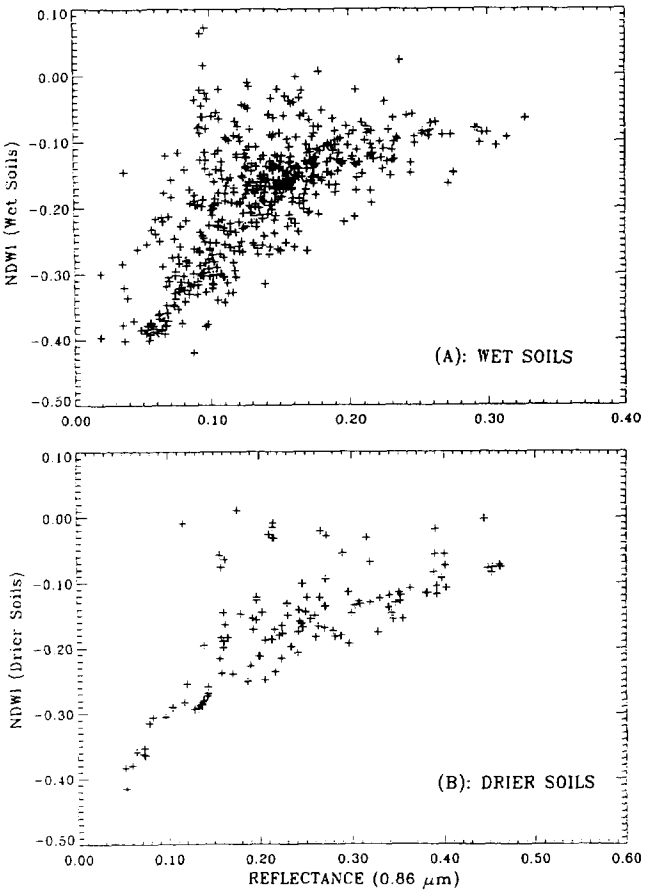

Figure 5. a) A scatter diagram between NDWI and the 0.86-μm reflectance for over 500 wet soils (Stoner and Baumgardner, 1980), and b) similar to a), but for approximately 130 drier soils.

NDWI for mixtures of all the wet soils with this vegetation (solid line) and the mean NDWI for mixtures of all the drier soils with this vegetation (dotted line) as a function of vegetation area fraction. Both curves show that the mean NDWI increases as the vegetation area fraction increases.

Atmosphere

The center wavelength positions of water vapor and liquid water bands in the 0.9–2.5 μm region are relatively shifted by approximately 50 nm. The shifts are due to O–H bonding strength differences for water in liquid phase and in gas phase. Figure 7 shows the atmospheric water vapor transmittance and liquid water transmittance as a function of wavelength. It is seen that the 0.86-μm and 1.24-μm channels used in NDWI are both located in atmospheric windows, where water vapor absorption is very small. In order to quantify the effects of atmospheric water vapor on NDWIs, the liquid water transmittance spectra in Figure 2 are multiplied by atmospheric water vapor transmittance spectra with total water vapor amounts between 0 and 30 cm. NDWIs are calculated from the resulting spectra. These NDWIs are compared with NDWIs for the pure liquid water cases. It is found that the largest errors introduced by atmospheric water vapor to NDWIs for liquid water thicknesses of 0.05 cm, 0.1 cm, 0.2 cm, and 0.4 cm are 1.50%, 0.74%, 0.37%, and 0.22%, respectively. Therefore, atmospheric water vapor effects on NDWIs are very small.

Atmospheric aerosols scatter and absorb solar radiation. The relative importance of aerosol scattering and absorption in remote sensing was previously investigated by Fraser and Kaufman (1985). In order to illustrate the atmospheric effects on NDWI and NDVI, radiative transfer calculations were performed using the 6S code (Vermote et al., 1996). The calculations were made for three narrow channels centered, respectively, at 0.66 μm, 0.865 μm, and 1.24 μm, for a solar zenith angle of 30°, and for a nadir looking geometry. The rural aerosol model with adjustable aerosol concentrations was used in the calculations. The assumed reflectances of surface vegetation at the three wavelengths were 0.03, 0.3, and 0.24, respectively. The true NDVI

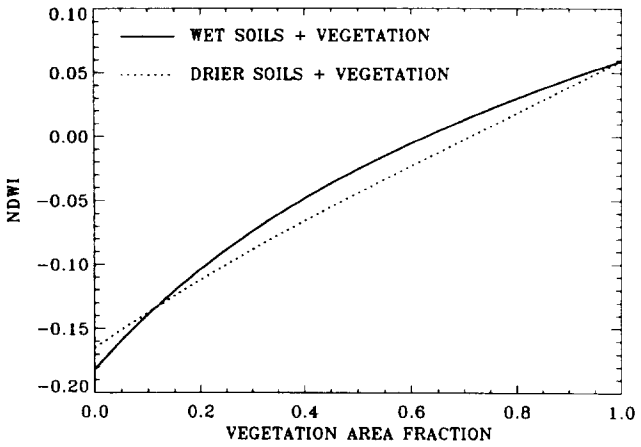

Figure 6. The mean NDWI for mixtures of wet soils with green vegetation (—) and the mean NDWI for mixtures of drier soils with green vegetation (····) as a function of vegetation area fraction (see text for more detailed descriptions).

value for this vegetation is 0.818, and the NDWI value is 0.107.

Figure 8a shows the resulting top-of-the-atmosphere apparent reflectances as a function of aerosol optical depths. For the curve of $\rho(0.66\ \mu m)$, the apparent reflectance increases as aerosol optical depth increases because of the dominant aerosol and molecular scattering effects. For the curves of $\rho(0.865\ \mu m)$ and $\rho(1.24\ \mu m)$, however, the apparent reflectances decrease as aerosol optical depth increases because of the dominant aerosol absorption effects over bright targets (Fraser and Kaufman, 1985). Figure 8b shows the NDWI (dashed line) and NDVI (solid line) as a function of aerosol optical depths. In order to see clearly the relative importance of aerosol effects on NDWI and NDVI, the two curves are scaled vertically so that the resulting new curves, also shown in Figure 8b, both have the same value of 1.0 at zero aerosol optical depth. It is seen that the scaled NDWI curve (dotted line) decreases much slower with increasing aerosol optical depth than the scaled NDVI curve (dash-dotted line). For aerosol optical depth increasing from 0 to 1.0, the NDWI decreased by 11%, and the NDVI by 34%. Therefore, NDWI is far less sensitive to atmospheric scattering effects than NDVI.

Figure 7. Sample water vapor and liquid water transmittance spectra. The positions and widths of two MODIS channels are marked as short thick horizontal bars in this figure.

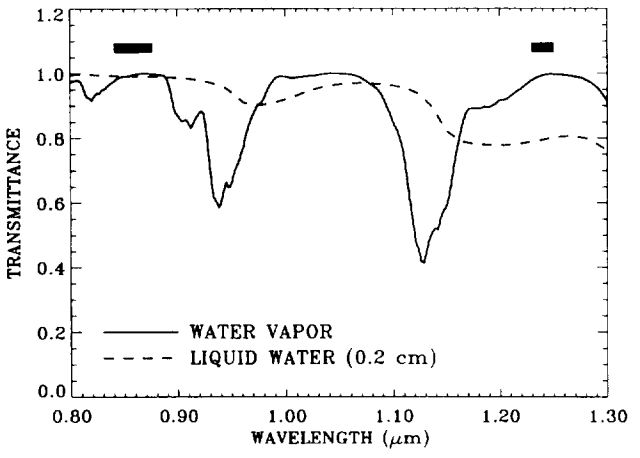

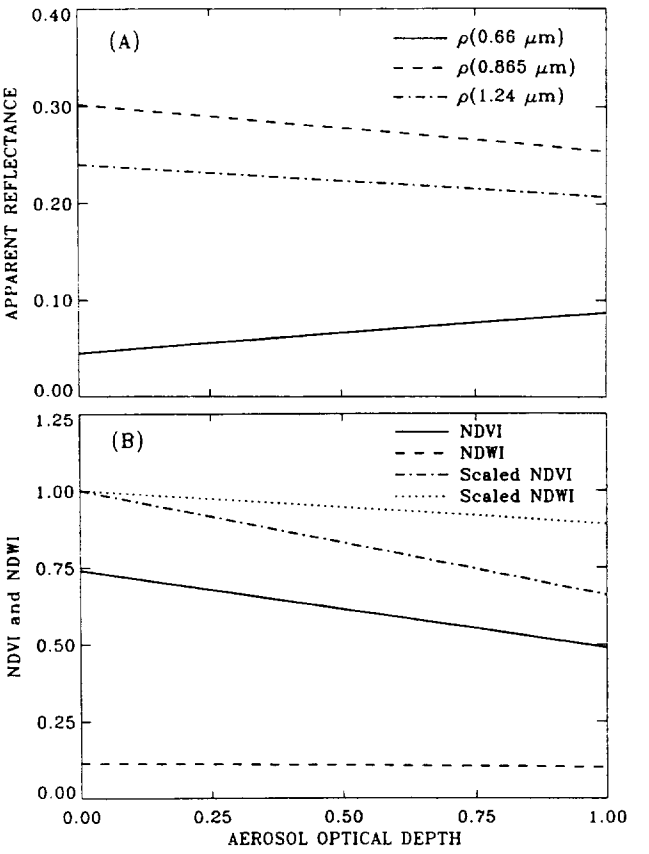

Figure 8. a) Top-of-the-atmosphere apparent reflectances as a function of aerosol optical depths for three channels at 0.66 μm, 0.865 μm, and 1.24 μm, and b) NDWI (---) and NDVI (—) as a function of aerosol optical depths. See text for detailed descriptions.

DEMONSTRATION WITH LABORATORY DATA

In the previous section the formulation of NDWI and effects of surface vegetation, soils and atmosphere on NDWI were described. In order to demonstrate the usefulness of NDWI for remote sensing of vegetation liquid water, the analysis of laboratory-measured reflectance spectra of stacked leaves are described in this section.

The laboratory measurements of reflectance spectra were made using a Beckman 5270 spectrometer attached

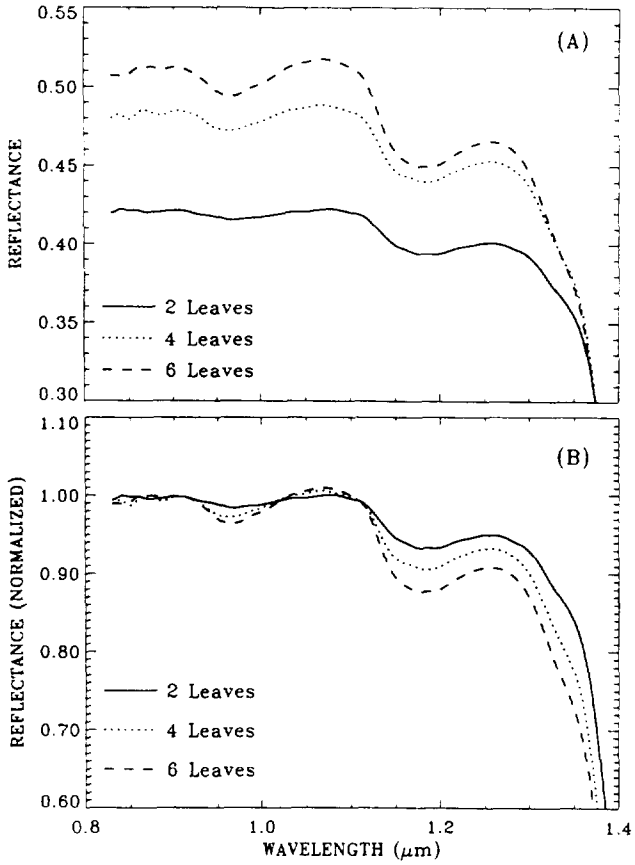

Figure 9. a) Laboratory-measured reflectance spectra over stacks of leaves with two, four, and six layers in the 0.8–1.4 μm region; b) similar to a), except that the spectra are normalized near 0.86 μm.

with an integrating sphere. Broad leaves picked from a small tree in a greenhouse were stacked inside a sample holder. The interior bottom and side surfaces of the holder were painted black in order to decrease the reflection and scattering from these surfaces. Figure 9a shows the measured reflectance spectra for stacks of leaves with two, four, and six leaf layers in the 0.8–1.4 μm region. As leaf layer increases, the absolute values of reflectances in the entire spectral region are increased. The weak liquid water absorption bands centered approximately at 0.98 μm and 1.20 μm are obviously seen from this figure. Figure 9b is similar to Figure 9a, except that the spectra are normalized near 0.86 μm. As the leaf layer increases, the reflectance near 1.24 μm relative to that near 0.86 μm is decreasing due to the increased liquid water absorption. Figure 10 shows NDWIs calculated from the measured spectra as a function of leaf layers. NDWIs increase as leaf layer increases—indicating that NDWI is sensitive to the total amounts of liquid water in the stacked leaves.

DEMONSTRATION WITH AVIRIS DATA

In order to further demonstrate the usefulness of NDWI for remote sensing vegetation liquid water from space,

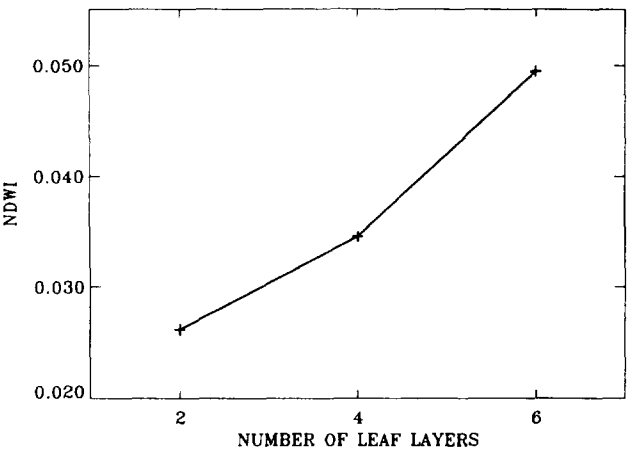

Figure 10. a) NDWIs calculated from the measured reflectance spectra as a function of leaf layers.

the analysis of spectral imaging data acquired with the NASA/Jet Propulsion Laboratory (JPL) Airborne Visible Infrared Imaging spectrometer (AVIRIS) (Vane et al., 1993) is described in this section. AVIRIS typically acquires data from an ER-2 aircraft at 20 km in 224 10-nm channels covering the complete 0.4–2.5 μm solar spectral region. Results from analysis of AVIRIS data measured over Jasper Ridge, California on 2 June 1992 and an area of the High Plains in northern Colorado on 7 August 1990 are presented below.

Jasper Ridge, California

Jasper Ridge is located west of the main campus of Stanford University, in the foothills of the Santa Cruz Mountains. It has been the site of biological investigations for more than 90 years and has numerous ongoing ecological and physiological studies (Elvidge et al., 1991). Figure 11a shows the false color NDVI image of the area, which covers a surface area of approximately 11 × 10 km. The color coding scheme used is that NDVI value changes continuously from 0.1 (blue) to 0.7 (red). The color bar in the bottom part of this figure illustrates the coding scheme. The upper left portion of the image covers areas with dead grass, and the right portion of the image covers areas with green vegetation. The spatial variation of the NDVI image over the green vegetation areas is small. Figure 11b shows the false color NDWI image (a mask was applied to water surface areas). The color coding scheme is illustrated in the bottom part of this figure. The NDWI values over areas with dead grass are negative, while those over green vegetation areas are positive. In addition, the NDWI image over green vegetation areas shows a number of "red" streaks related to the drainage patterns. These streaks, or drainage patterns, are almost completely absent in the NDVI image. This indicates that NDWI is sensitive to liquid water in vegetation.

A scatter diagram of NDVI versus NDWI for all

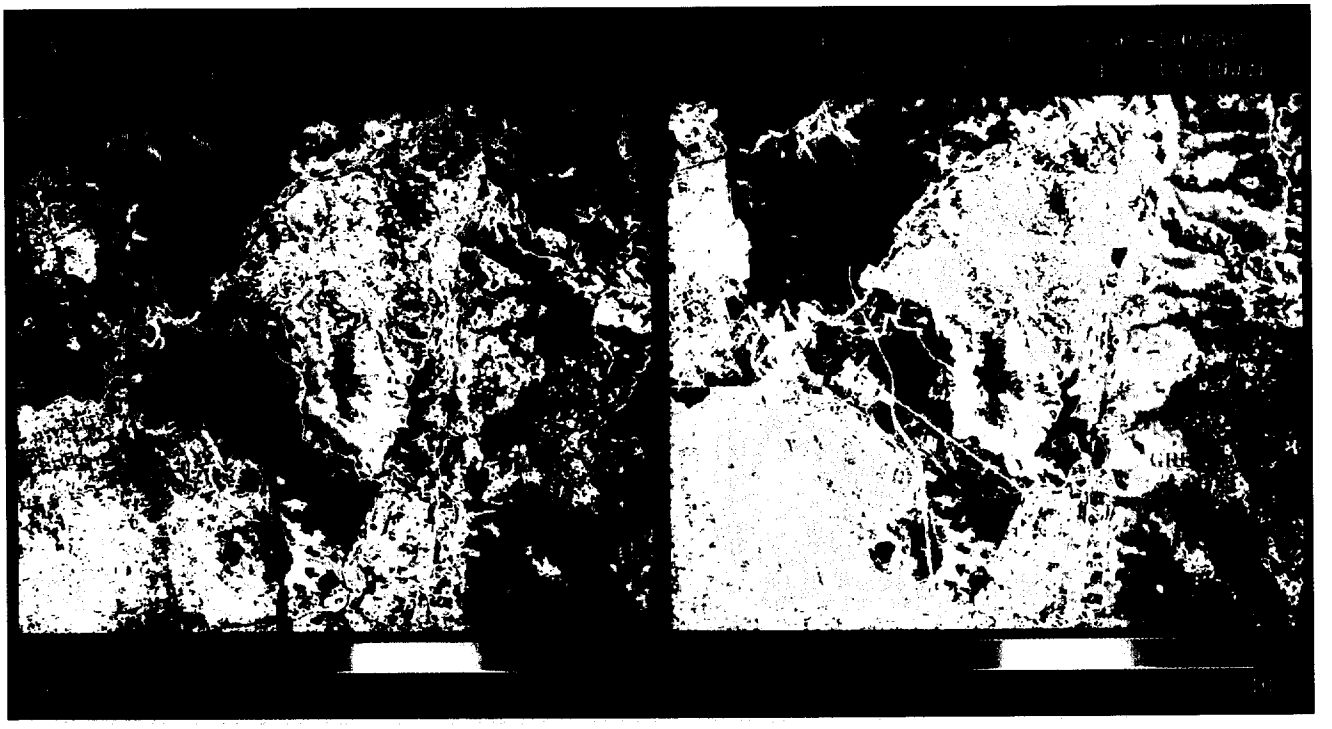

Figure 11. Images of NDVI (a) and NDWI (b) calculated from spectral imaging data acquired with AVIRIS over Jasper Ridge, California on 2 June 1992.

green vegetation pixels with NDVI greater than 0.4 is shown in Figure 12. Many points with NDWI values between 0 and 0.15 have similar NDVI values (approximately 0.63). This is consistent with the fact that the spatial variation of the NDVI image over green vegetation areas in Figure 11a is small, while the spatial variation of the NDWI image over the same vegetated areas in Figure 11b is large. In order to see more quantitatively the relationship between NDVI and NDWI, the points in Figure 12 are grouped at an equal NDWI interval of 0.01. The mean and standard deviation of NDVI values within each NDWI interval are calculated. The solid line is the curve of mean NDVI as a function of NDWI, and the two dashed lines are the curves of mean NDVIs plus and minus 1 standard deviation. The mean curve shows that for NDVI values between approximately 0.55 and 0.62, NDVI increases linearly with NDWI. However, when NDVI reaches about 0.63, it is almost constant with NDWI. This demonstrates that, at large NDVI values, NDVIs are saturated while NDWIs remain sensitive to liquid water in green vegetation.

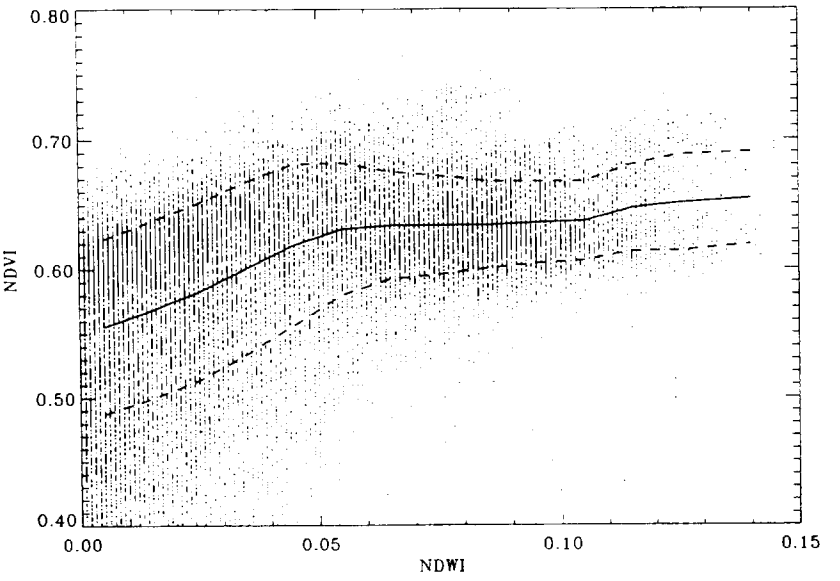

Figure 12. A scatter diagram of NDVI versus NDWI for all green vegetation pixels in the Jasper Ridge image with NDVIs greater than 0.4. The solid line is the curve of mean NDVI as a function of NDWI, and the two dashed lines are the curves of mean NDVIs plus and minus 1 standard deviation. See text for more detailed descriptions.

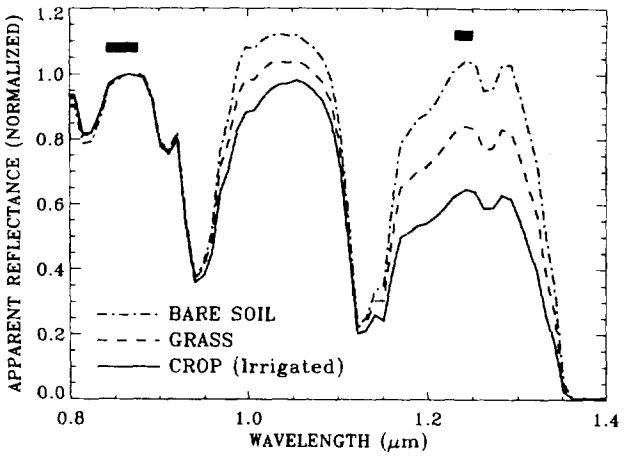

Figure 13. Samples of apparent reflectance spectra (normalized near 0.86 μm) measured with AVIRIS over areas covered by bare sandy soils, natural grasses, and irrigated crops.

Clear water surface reflectances beyond 0.7 μm are close to zero. Because Rayleigh scattering effect varies inversely with the fourth power of wavelength, NDWIs derived from AVIRIS images over clear water surfaces can be as large as 0.63, which is greater than most NDWIs over areas covered by green vegetation. This is the case for NDWIs calculated from the AVIRIS' Jasper Ridge images. A mask was applied to the original NDWI image so that lakes in Figure 11b appeared dark.

High Plains, Colorado

Another data set used in this study is the AVIRIS data acquired over an area (40°20'N and 104°16'W) of the High Plains in northern Colorado, approximately 50 km north of Denver (Yuhas et al., 1993). This data set was acquired during the vegetation peak growing season. The imaging scene contains areas covered by sandy soils (almost no vegetation), natural grass, and irrigated farms. Examples of apparent reflectance spectra (normalized near 0.86 μm) over areas covered by sandy soil, natural grass (no irrigation system), and well-irrigated crop are shown in Figure 13. It is seen that, from bare soil to natural grass and then to crop, the 1.24 μm reflectance (relative to 0.86 μm) progressively decreases. The NDWI values calculated from the spectra of bare soil, grass, and crop are -0.022, 0.084, and 0.215, respectively. Using the relationship between NDWI and liquid water thickness shown in Figure 3, the NDWI values from the grass and crop spectra are converted to equivalent liquid water thicknesses, which are 0.15 and 0.40 cm, respectively. The nonlinear least squares spectrum-matching technique (Gao and Goetz, 1995) have also been used for the retrieval of EWTs from the grass and crop spectra. The derived EWT values are 0.18 cm and 0.40 cm, respectively. EWT values obtained with both methods are approximately the same.

Figure 14a shows the NDVI image of the site. A segment of South Platte River is seen. Most of the area to the right of the river is covered by sandy soils. The dominant vegetation community here is short grass prairie, which is used primarily for grazing. NDVI values in this area are less than 0.4. The soils along the terraces of the river range from clay loams to clay. These soils are used for commercial dryland and irrigated farming (Yuhas et al., 1993). The NDVI values over the farming areas to the left of the river are mostly between 0.4 and 0.85. The fractional vegetation cover of each pixel within the scene varies from 0% (heavily grazed sandy areas) to 100% (well-irrigated farming areas).

Figure 14b shows the NDWI image of the scene. Most of the nonfarming areas have negative NDWI values, while farming areas have positive NDWI values. Major spatial patterns seen in Figure 14a are also seen in Figure 14b. The detailed spatial patterns in Figures 14a and 14b are, however, different. The histograms (not shown here) of NDVI and NDWI images have been examined. It is found that the NDVI image has significantly more pixels peaked at the high end of NDVI and less pixels in the middle range of NDVI in comparison with the NDWI image. As a result, the NDVI image in Figure 14a has more "red" pixels resulted from the saturation effect described previously, while the NDWI image in Figure 14b has more "yellow" pixels. Figures 13 and 14b have shown that NDWI records different information about vegetation condition than NDVI.

DISCUSSION AND SUMMARY

A new vegetation index, the normalized difference water index (NDWI), is proposed for remote sensing of vegetation liquid water from space. This index uses two narrow channels centered near 0.86 μm and 1.24 μm. Both channels sense similar depths through vegetation canopies, unlike the two channels used in NDVI. NDWI is a measure of liquid water molecules in vegetation canopies that interacted with the incoming solar radiation. It is less sensitive to atmospheric scattering effects than NDVI. A simple test of this index using laboratory-measured reflectance spectra of stacked leaves shows that NDWIs increase as leaf layer increases—indicating NDWI is sensitive to the total amounts of liquid water in the stacked leaves. Limited tests of this index using two sets of AVIRIS data demonstrated that NDWI images contain information independent of NDVI images. NDWI does not remove completely the soil background reflectance effects (see Figs. 5 and 6), similar to NDVI. It is possible to infer EWTs from NDWIs over areas fully covered by green vegetation. However, it is difficult to do so from NDWIs over partially vegetated areas, because soil contributions to NDWIs are mostly negative, whereas green vegetation contributions are positive. In order to gain improved understanding of its usefulness and limitations, NDWI should be further

Figure 14. Images of NDVI (a) and NDWI (b) calculated from spectral imaging data acquired with AVIRIS over an area in the High Plains in northern Colorado.

tested with laboratory and field measured reflectance spectra of vegetation canopies. Rigorous radiative transfer modeling at both the leaf level and the canopy level will also help to understand this index. Because the information about vegetation canopies contained in the 1.24-μm channel is very different from that contained in the red channel near 0.66 μm, NDWI should be considered as an independent vegetation index. It is complementary to, not a substitute for NDVI. The next generation of satellite instruments, such as Landsat 8 and MODIS, will have channels centered at 1.24 μm. Ecologists and biologists are encouraged to develop new techniques to extract information about vegetation canopies from the 1.24-μm channels.

The author is grateful to R. O. Green of the Jet Propulsion Laboratory and to R. Yuhas of University of Colorado in Boulder, Colorado for providing AVIRIS data, to B. Curtiss of University of Colorado at Boulder and to C. D. Elvidge of Desert Research Institute in Reno, Nevada for providing laboratory-measured vegetation reflectance spectra, to L. Biehl of Purdue University for providing the soil reflectance spectra used in this article, and to J. Irons, Y. J. Kaufman, and R. S. Fraser at NASA Goddard Space Flight Center for useful comments on this article.

REFERENCES

Bowker, D. E., Davis, R. E., Myrick, D. L., Stacy, K., and Jones, W. T. (1985), Spectral reflectances of natural targets for use in remote sensing studies, NASA Ref. Publ. 1139, Washington, DC.

Bowman, W. D. (1990), The relationship between leaf water status, gas exchange, and spectral reflectance in cotton leaves. *Remote Sens. Environ.* 31:249–255.

Cibula, W. G., Zetka, E. F., and Rickman, D. L. (1992), Response of thematic bands to plant water stress. *Int. J. Remote Sens.* 13:1869–1880.

Deering, D. (1989), Field measurements of bidirectional reflectance, in *Theory and Applications of Optical Remote Sensing* (G. Asrar, Ed.), Wiley, New York, pp. 14–65.

Elvidge, C. D. (1990), Visible and near infrared reflectance characteristics of dry plant materials, *Int. J. Remote Sens.* 11:1775–1795.

Elvidge, C. D., Chen, Z. K., and Groeneveld, D. P. (1991), Detection of trace quantities of green vegetation in AVIRIS data, JPL Publication 91-28, Pasadena, CA, pp. 183–188.

Fraser, R. S., and Kaufman, Y. J. (1985), The relative importance of aerosol scattering and absorption in remote sensing. *IEEE Trans. Geosci. Remote Sens.* GE-23:615–633.

Gao, B.-C. (1995), A normalized difference water index for remote sensing of vegetation liquid water from space, in *SPIE's 1995 Symposium on OE / Aerospace Sensing and Dual Use Photonics*, Vol. 2480, Orlando, FL.

Gao, B.-C., and Goetz, A. F. H. (1994), Extraction of dry leaf spectral features from reflectance spectra of green vegetation. *Remote Sens. Environ.* 47:369–374.

Gao, B.-C., and Goetz, A. F. H. (1995), Retrieval of equivalent water thickness and information related to biochemical components of vegetation canopies for AVIRIS data. *Remote Sens. Environ.* 52:155–162.

Goetz, A. F. H., Vane, G., Solomon, J., and Rock, B. N. (1985),

Imaging spectrometry for earth remote sensing. *Science* 228:1147–1153.

Hunt, E. R., Jr., and Rock, B. N. (1989), Detection of changes in leaf water content using near- and middle-infrared reflectances. *Remote Sens. Environ.* 30:43–54.

Hunt, E. R., Jr., Rock, B. N., and Nobel, P. S. (1987), Measurement of leaf relative water content by infrared reflectance. *Remote Sens. Environ.* 22:429–435.

Jackson, R. D., Slater, P. N., and Pinter, P. J., Jr. (1983), Discrimination of growth and water stress in wheat by various vegetation indices through clear and turbid atmospheres, *Remote Sens. Environ.* 13:187–208.

Kaufman, Y. J., and Tanré, D. (1992), Atmospherically resistant vegetation index (ARVI) for EOS-MODIS, *IEEE Trans. Geosci. Remote Sens.* 30:261–270.

Lillesaeter, O. (1982), Spectral reflectance of partly transmitting leaves: laboratory measurements and mathematical modeling. *Remote Sens. Environ.* 12:247–254.

Palmer, K. F., and Williams, D. (1974), Optical properties of water in the near infrared, *J. Opt. Soc. Am.* 64:1107–1110.

Pierce, L. L., Running, S. W., and Riggs, G. A. (1990), Remote detection of canopy water stress in coniferous forests using the NS001 thematic mapper simulator and the thermal infrared multispectral scanner, *Photogramm. Eng. Remote Sens.* 56:579–586.

Salomonson, V. V., Barnes, W. L., Maymon, P. W., Montgomery, H. E., and Ostrow, H. (1989), MODIS: advanced facility instrument for studies of the earth as a system. *IEEE Trans. Geosci. Remote Sens.* 27:145–153.

Stoner, E. R., and Baumgardner, M. F. (1980), Physiochemical, site and bidirectional reflectance factor characteristics of uniformly moist soils, NASA CR-160571, pp. 1–50.

Tucker, C. J. (1980), Remote sensing of leaf water content in the near-infrared, *Remote Sens. Environ.* 10:23–32.

Tucker, C. J., Justice, C. O., and Pince, S. D. (1986), Monitoring the grasslands of the Sahel 1984–1985, *Int. J. Remote Sens.* 7:1571–1581.

Vane, G., Green, R. O., Chrien, T. G., Enmark, H. T., Hansen, E. G., and Porter, W. M. (1993), The Airborne Visible Infrared Imaging Spectrometer, *Remote Sens. Environ.* 44(2 / 3):127–143.

Vermote, E., Tanré, D., Deuze, J. L., Herman, M., and Morcrette, J. J. (1996), Second simulation of the satellite signal in the solar spectrum: an overview. *IEEE Trans. Geosci. Remote Sens.*, (in press).

Yuhus, R. H., Boardman, J. W., and Goetz, A. F. H. (1993), Determination of semi-arid landscape endmembers and seasonal trends using convex geometry spectral unmixing techniques, JPL Publication 93-26, Jet Propulsion Lab., Pasadena, CA, pp. 205–208.